LA-UR-22-20292

Approved for public release; distribution is unlimited.

Title:	The Bouger's Law Shell Ionospheric Transfer Function
Author(s):	Light, Max Eugene
Intended for:	Report
Issued:	2022-01-13

The Bouger's Law Shell Ionospheric Transfer Function

Max Light

January 4, 2022

1 Introduction

Ionospheric transfer function (ITF) algorithms determine the effects of the ionosphere on an electromagnetic (EM) radio-frequency (RF) signal as it propagates through. In this report, the Bouger's law shell model is outlined. This ITF is very similar to the Snell's Law Shell ITF [1]; however, in this formulation, plasma parameters in the ionosphere are allowed to change radially.

This algorithm is expressed in the frequency domain. In this way, it is applied as linear time invariant (LTI) filter function [2].

Signals in this report are assumed to have only a single component (i.e. x, y or z in a rectangular coordinate system). Multi-component signals can be treated simply by applying the specific ITF to each component separately.

Contents

2 Review of Snell's law

2.1 inhomogeneous media - stratified layers

2.1.1 rectilinear stratification

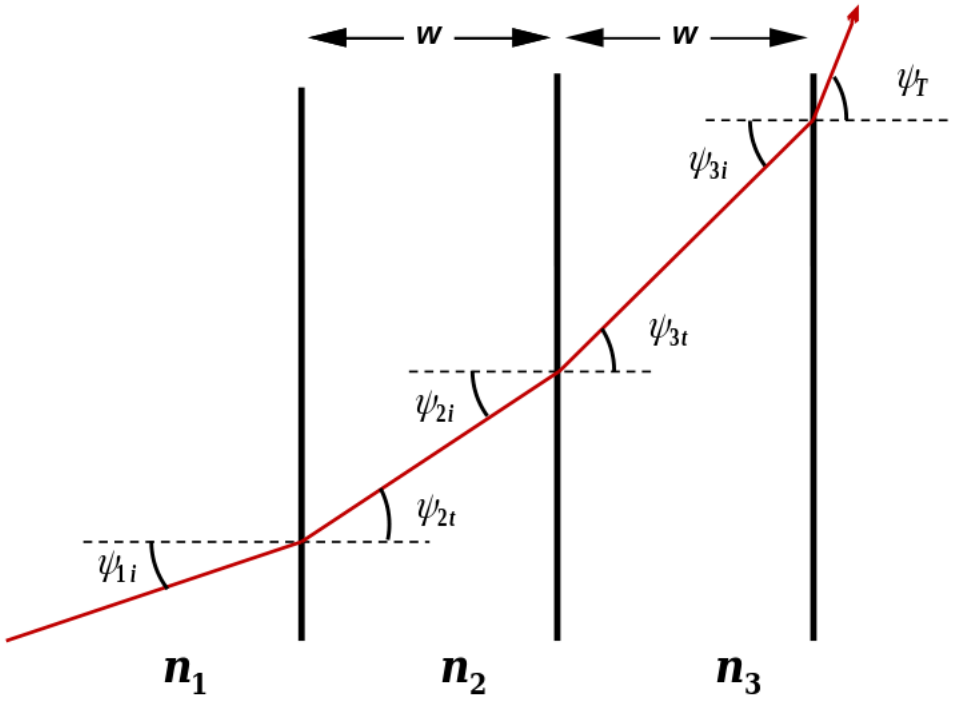

Figure 1: Geometry for Snell's law in a rectilinear planar stratified medium.

Consider an EM wave propagating in a planar stratified medium, with each layer having a width w, as shown in Fig. 1. Here, the properties of each layer are homogeneous, but from one to the next they can change. Their respective refractive indices are $\mathfrak{n}_1, \mathfrak{n}_2$, and $\mathfrak{n}_3$. The EM wave propagates from medium 1 through 3 (and beyond). We assume it propagates under the constraints of geometric optics [3, 4], and furthermore will neglect reflections at boundaries. Snell's law relates the incident to transmitted angles as

$$\mathfrak{n}_1 \sin\psi_{1i} = \mathfrak{n}_2 \sin\psi_{2t} = \mathfrak{n}_3 \sin\psi_{3t} = K \tag{1}$$

or

$$\mathfrak{n}_j \sin\psi_{ji} = K \tag{2}$$

Note that due to the geometry, incident and transmitted angles are equal inside each stratified layer. Thus, we can calculate the angle of transmission into a fourth layer from, say, information of the first layer alone

$$\sin\psi_T = \frac{K}{\mathfrak{n}_4} = \frac{\mathfrak{n}_1}{\mathfrak{n}_4}\sin\psi_{1i} \tag{3}$$

The path length of the ray through each layer is straightforward to calculate from geometry

$$S_j = \frac{w}{\cos\psi_{jt}} \tag{4}$$

and the total path length through the medium is simply the sum

$$S_{total} = \sum_j S_j \tag{5}$$

2.1.2 polar stratification

Next, consider the same situation in a polar stratified medium, as shown in Fig. 2.

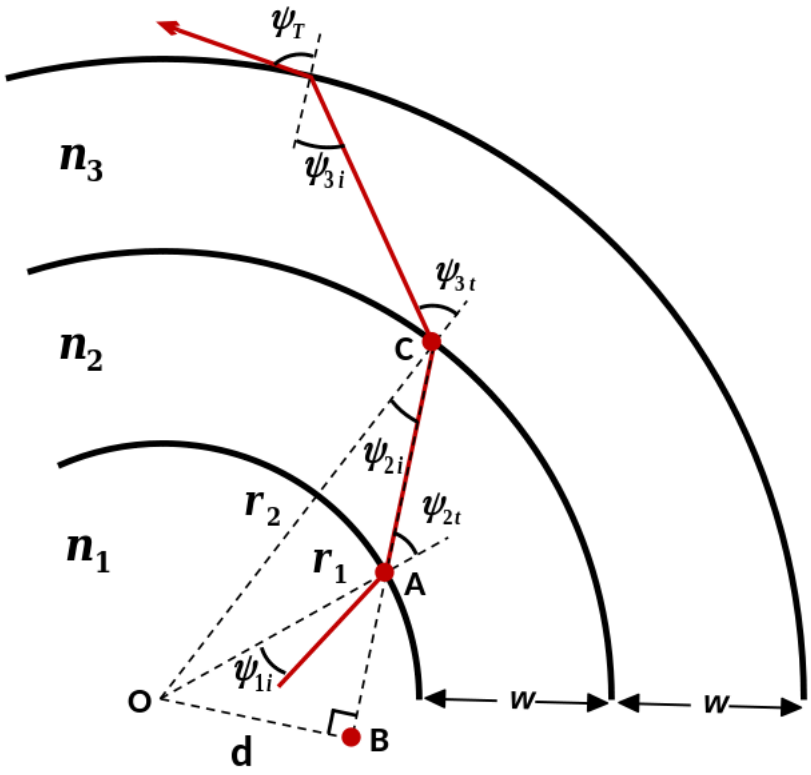

Figure 2: Geometry for Snell's law in a polar stratified medium.

The boundaries of each layer are defined by their radii with respect to the point O. The EM wave starts in layer 1, and refracts through layer 3 (again ignoring reflections at boundaries), where each layer is defined by a thickness w. Here, the system geometry dictates that transmitted and incident angles within each layer are no longer equal, that is

$$\psi_{2t} \neq \psi_{2i} \qquad \psi_{3t} \neq \psi_{3i} \tag{6}$$

so we must take a different path to reach a relation like Eq. 2.

Consider the right triangle OBC in Fig. 2. The leg BC is coliniear with the ray path in the second layer. Notice that this triangle shares leg d with right triangle OBA. From this construction, we see that the angles ψ_{2t} and ψ_{2i} are related by

$$\sin\psi_{2t} = \frac{d}{r_1} \quad = \quad \sin\psi_{2i} = \frac{d}{r_2} \quad \Longrightarrow r_1 \sin\psi_{2t} = r_2 \sin\psi_{2i} \tag{7}$$

Furthermore, from geometric optics, we can apply Snell's law locally. At point A this gives

$$\mathfrak{n}_1 \sin\psi_{1i} = \mathfrak{n}_2 \sin\psi_{2t} \tag{8}$$

or, using $\sin\psi_{2t}$ from Eq. 7

$$r_2\mathfrak{n}_2 \sin\psi_{2i} = r_1\mathfrak{n}_1 \sin\psi_{1i} \tag{9}$$

which is generalized for all layers as in Eq. 2

$$r_j\mathfrak{n}_j \sin\psi_{ji} = K \tag{10}$$

Now we can relate incident angles in each layer through Eq. 10, and transmitted angles with Eq. 2 using parameters of the two layers encompassing the boundary of interest. Eqn. 10 is known as Bouger's law [3] for EM waves propagating in spherically stratified media.

Here, to find the transmitted angle ψ_T into medium 4, we get

$$\sin\psi_T = \frac{\mathfrak{n}_3}{\mathfrak{n}_4}\sin\psi_{3i} = \frac{\mathfrak{n}_3}{\mathfrak{n}_4}\frac{K}{r_3\mathfrak{n}_3} = \frac{r_1}{r_3\mathfrak{n}_4}\sin\psi_{1i} \tag{11}$$

The path length through each layer can again be calculated from geometry. Consider the ray's path S_2 through layer 2 in Fig. 2 from points A to C. From triangles OAB, OCB, and the Law of sines, we get

$$S_2 = r_2\,\frac{\sin(\psi_{2t}-\psi_{2i})}{\sin\psi_{2t}} \tag{12}$$

or, more generally

$$S_j = r_j\,\frac{\sin(\psi_{jt}-\psi_{ji})}{\sin\psi_{jt}} \tag{13}$$

where

$$r_j = jw \tag{14}$$

and the total path length through the stratified medium is given in Eq. 5.

2.2 inhomogeneous media - continuous variation

If each layer were made infinitesimally thin, we can think of the medium through which the EM wave propagates (ionosphere) as a single shell with refractive parameters that vary continuously. While the rectilinear and polar geometric form of Snell's law, Eqns. 2 and 10, still hold, calculation of the respective path lengths changes from discrete to differential. The path length is critical in that it is used to determine the phase change imparted by the ionosphere on the propagating EM wave.

2.2.1 rectilinear geometry

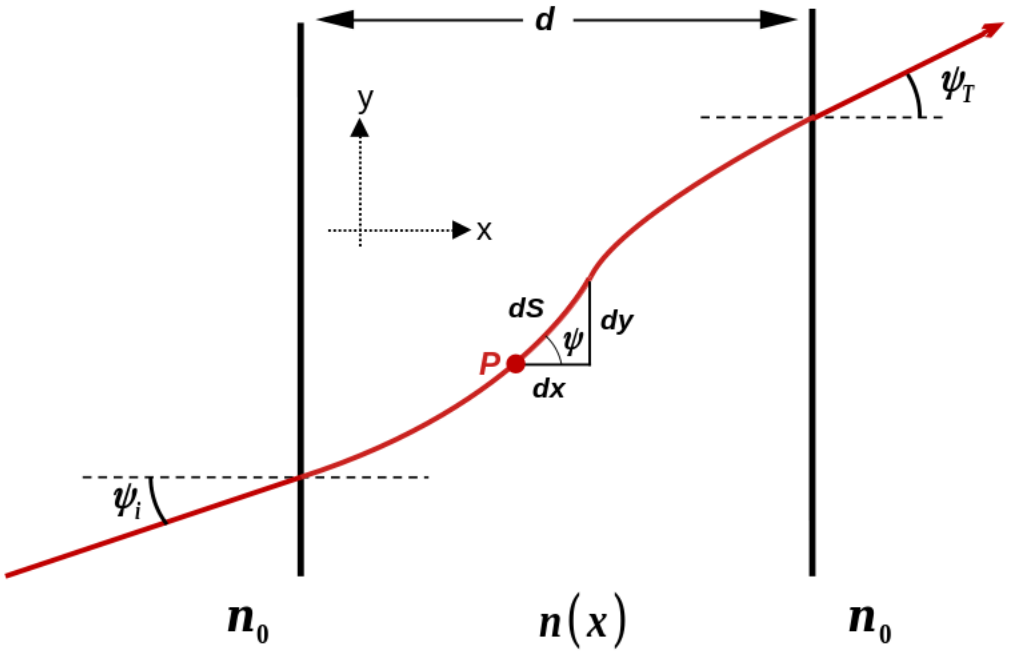

Figure 3: Geometry for Snell's law in an inhomogeneous medium where the refractive index $\mathfrak{n}$ is a function of x only.

Consider the situation shown in Fig. 3. An EM wave is incident from a medium with refractive index $\mathfrak{n}_0$ to a medium in which it changes with respect to the x coordinate ($\mathfrak{n} \longrightarrow \mathfrak{n}(x)$). At point P the ray will continue a distance dS at an angle ψ, which is the angle of transmission. Thus, from Snell's law,

$$\mathfrak{n}(x) \sin\psi = \mathfrak{n}_0 \sin\psi_i = K \tag{15}$$

or

$$\sin\psi = \frac{K}{\mathfrak{n}(x)} \tag{16}$$

where $K = \mathfrak{n}_0 \sin\psi_i$. Furthermore, from the differential triangle at point P we see that

$$\cos\psi = \frac{dx}{dS} \tag{17}$$

thus

$$\frac{dx^2}{dS^2} + \frac{K^2}{\mathfrak{n}^2(x)} = 1 \tag{18}$$

The differential path length dS is then

$$dS = \frac{\mathfrak{n}(x)}{\sqrt{\mathfrak{n}^2(x) - K^2}}\, dx \tag{19}$$

and we can find the total path length through the medium by integration

$$S = \int_0^d \frac{\mathfrak{n}(x)}{\sqrt{\mathfrak{n}^2(x) - \mathfrak{n}_0^2 \sin^2 \psi_i}}\, dx \tag{20}$$

2.2.2 polar geometry

In this situation, The EM wave (ray) is incident at point A and emerges at point B. The refractive index varies continuously in radius ($\mathfrak{n} \longrightarrow \mathfrak{n}(r)$), causing a continuous variation in the ray's direction as a function of radius.

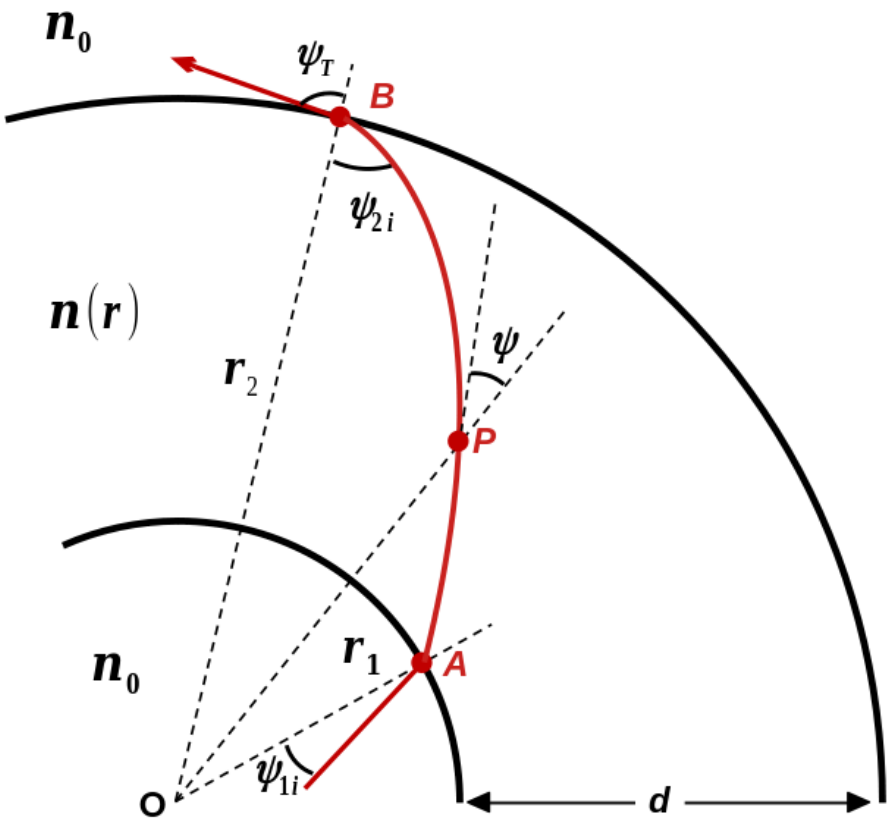

Figure 4: Geometry for Snell's law in an inhomogeneous medium in which $\mathfrak{n}$ is a function of r only.

The path length S from A to B can be solved using analytic geometry. Consider the curve in Fig. 5 of the form $r = f(\theta)$, where r is a differentiable function of θ, and let it represent the EM ray's path through an inhomogeneous medium.

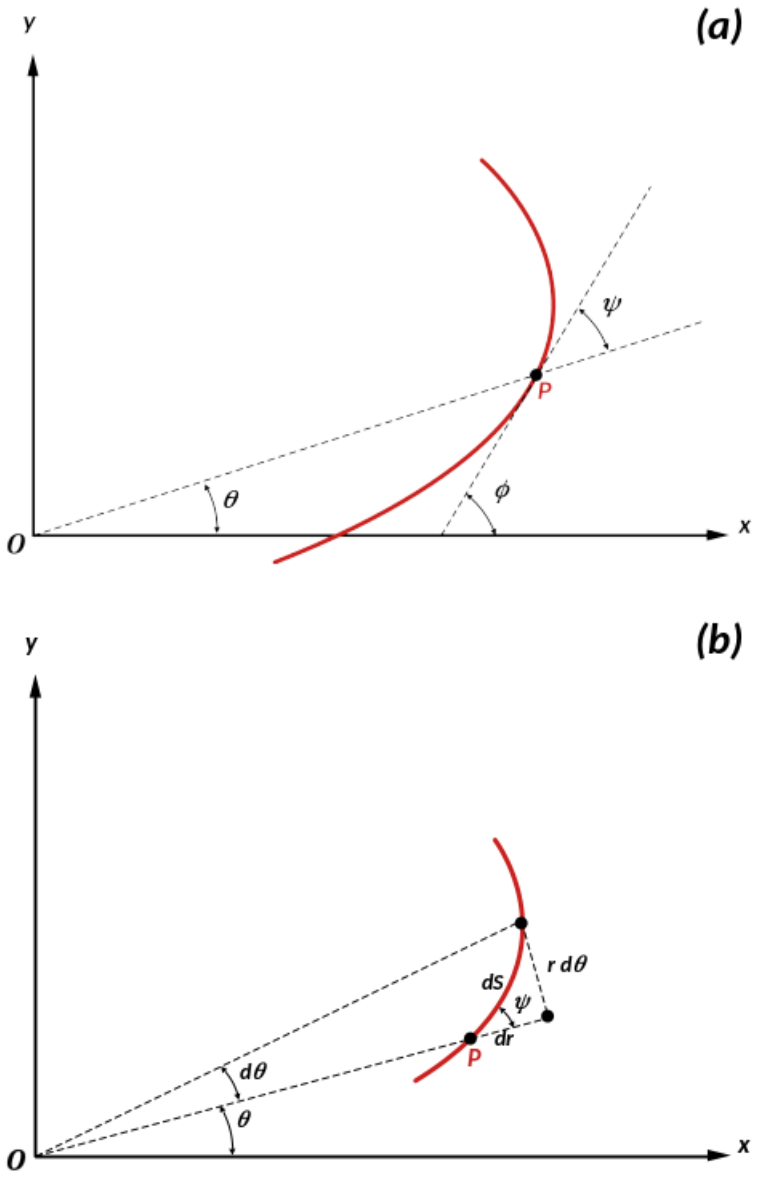

Figure 5: Angle ψ between the tangent and radius vector.

At any point P on that curve, the relationship between the polar angle θ, tangential angle ϕ [5], and the angle ψ between the radius and tangent to that point is (Fig. 5a)

$$\phi = \theta + \psi \tag{21}$$

Notice that the angle ψ is equivalent to the angle ψ_T in Fig. 4, or any transmission angle ψ interior to the medium. We would like to solve for this along with the differential path length dS.

To find ψ, recall

$$x = r\cos\theta \qquad y = r\sin\theta \tag{22}$$

where

$$\frac{dx}{d\theta} = -r\sin\theta + \cos\theta\frac{dr}{d\theta} \tag{23}$$

$$\frac{dy}{d\theta} = r\cos\theta + \sin\theta\frac{dr}{d\theta} \tag{24}$$

From Eq. 21

$$\tan\psi = \tan(\phi-\theta) = \frac{\tan\phi - \tan\theta}{1+\tan\phi\tan\theta} \tag{25}$$

The definitions of θ and ϕ are [5]

$$\tan\theta = \frac{y}{x} \qquad \tan\phi = \frac{dy/d\theta}{dx/d\theta} \tag{26}$$

from which we can find a form of ψ more tractable for polar geometry

$$\tan\psi = \frac{r}{dr/d\theta} \tag{27}$$

The differential element of path length is solved from Eqns. 23 and 24

$$dS = \left[dx^2+dy^2\right]^{1/2} = \left[r^2d\theta^2+dr^2\right]^{1/2} \tag{28}$$

which can also be verified from the differential triangle in Fig. 5b.

We integrate Eqn. 28 to get the total path length

$$S = \int dS = \int \left[r^2\left(\frac{d\theta}{dr}\right)^2 + 1\right]^{1/2} dr \tag{29}$$

using the functional form of $r = f(\theta)$ in the integrand.

3 Bouger's law ITF

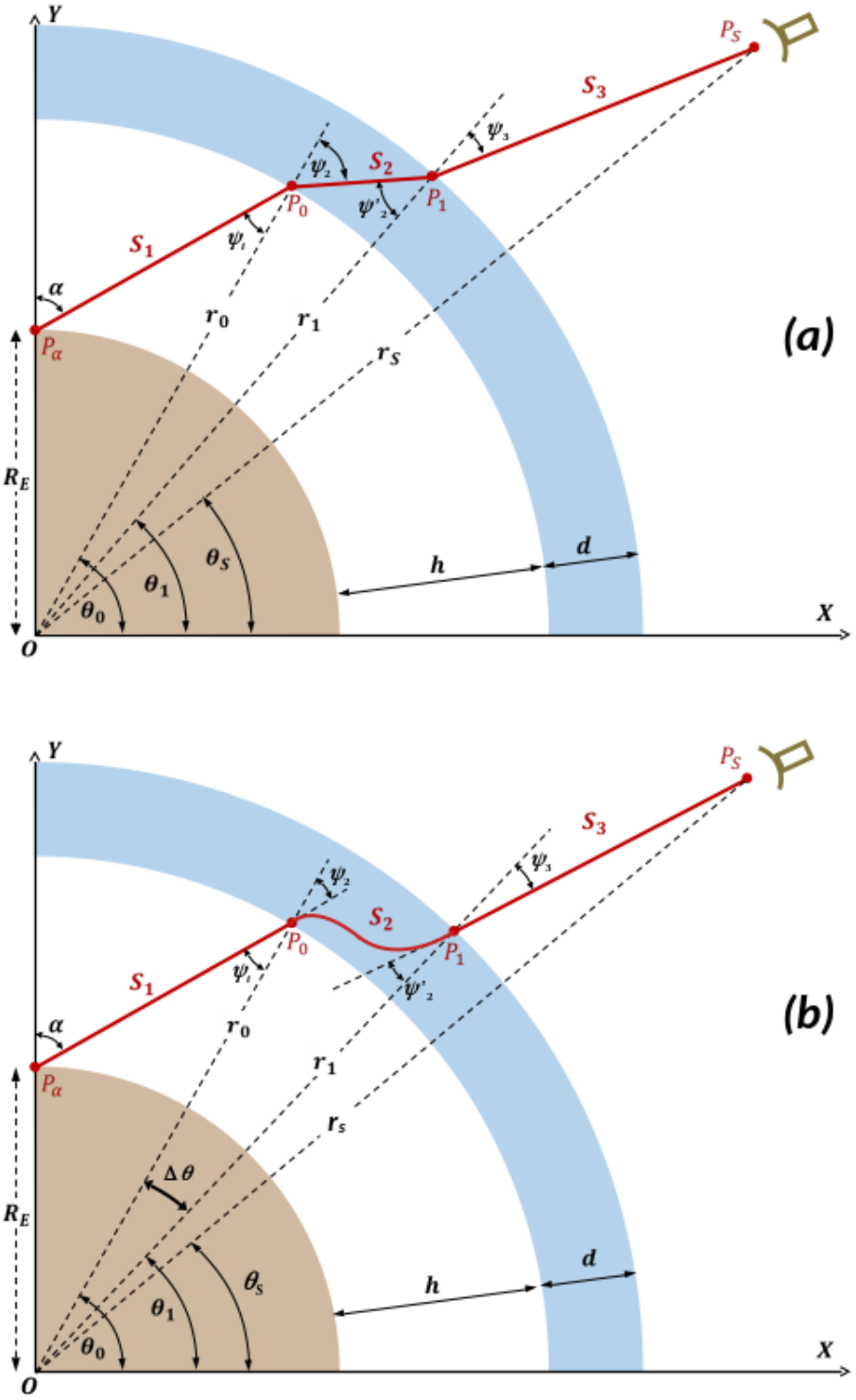

Figure 6: Geometry for the Snell and Bouger's law ITF models. The configuration for a ray that hits the satellite is shown. (a) Snell's law shell; (b) Bouger's law shell.

This ITF is quite similar to the Snell's law ITF [1] except for one important difference. Here, the EM wave ray that traverses the ionosphere will have a path that continually changes direction due

to the continuous variation in the ionospheric refractive index $\mathfrak{n}$ in the radial direction, as shown in Fig. 6(b). We are restricting $\mathfrak{n}$ to vary in the *radial* direction only.

Consider an EM signal originating at a point source and traversing the ionosphere to a detector, as shown in figure 6. The ionosphere is represented by the blue region and is assumed to be an inhomogeneous spherical shell of some arbitrary thickness d, starting at a radius h relative to the earth's surface at radius R_E. The plasma electron density will have some radial profile. Electron collisions and ion motions will be ignored in this treatment because ions are considered to be too massive to contribute to phenomena on the time scale of the RF EM wave, and wave damping due to electron collisions is assumed insignificant. In rectilinear coordinates, the signal path is

$$P_\alpha(0, R_E) \longrightarrow P_0(x_0, y_0) \longrightarrow P_1(x_1, y_1) \longrightarrow P_S(x_S, y_S) \tag{30}$$

or in cylindrical coordinates

$$P_\alpha(R_E, \pi/2) \longrightarrow P_0(r_0, \theta_0) \longrightarrow P_1(r_1, \theta_1) \longrightarrow P_S(r_S, \theta_S) \tag{31}$$

It travels a total distance $S = S_1 + S_2 + S_3$. Thus, the signal amplitude is decreased by a factor $1/S$. This is not strictly correct, as it does not account for the increase in the flux tube encompassed by the ray as it propagates outward in the r coordinate. However, for the purposes of this report, this assumption is strong enough to be considered valid for the change in signal amplitude.

Note also that, by definition, the ray will refract such that $\theta_1 < \theta_0$ always because the presence of a plasma will cause it to bend clockwise away from the radial direction. This is also true if there were no plasma present by geometry. Thus, referring to Fig. 6(b)

$$\theta_1 = \theta_0 - \Delta\theta \tag{32}$$

The Earth's magnetic field magnitude B_0 and angle relative to the ray direction β are constant. β is set by the angle between the LOS of the incident ray at the ionospheric underside, and B_0 can correspond to its maximum amplitude within the ionosphere. If these quantities were allowed to change radially in addition to the plasma electron density, the ITF calculation would need to be done using the ray tracing method due to the fact that the EM ray direction relative to the magnetic field's orientation would need to be known at each step through the ionosphere to calculate β. Thus, knowledge of the ray's path would be necessary *before* it was calculated.

To summarize, the assumptions used above are

- PLASMA The ionosphere is a shell of plasma with a radial density profile, containing massive ions and collisionless electrons.
- MAGNETIC FIELD The Earth's magnetic field is a constant.
- B_0 ORIENTATION The angle between the Earth's magnetic field and the line of sight does not change.

The index of refraction $\mathfrak{n}_p(r, \omega)$ in the plasma for either fast ($\mathtt{m} = -1$) or slow ($\mathtt{m} = +1$) root is given by the Appleton Hartree dispersion relation [3]

$$\mathfrak{n}_p(r,\omega) = \sqrt{1 - \frac{X(r,\omega)}{1 - \frac{1}{2}\frac{Y^2(\omega)\sin^2\beta}{1 - X(r,\omega)} + \mathtt{m}\left[\frac{1}{4}\frac{Y^4\sin^4\beta}{(1 - X(r,\omega))^2} + Y^2(\omega)\cos^2\beta\right]^{1/2}}} \tag{33}$$

where

$$X(r,\omega) = \frac{\omega_p^2(r,\omega)}{\omega^2} \qquad Y(\omega) = \frac{\omega_c}{\omega} \tag{34}$$

The plasma and cyclotron frequencies are

$$\omega_p^2(r) = \frac{n_0(r)q^2}{\epsilon_0 m_e} \quad \text{and} \quad \omega_c = \frac{qB_0}{m_e} \tag{35}$$

where ϵ_0, m_e, and q are the permittivity of free space, electron mass, and electron charge in MKS units respectively. Note that parameters depending on plasma density n_0 are functions of radius.

In addition, a two dimensional geometry is constructed so that the source is located at point P at $(r,\theta) = (R_E, \pi/2)$ where R_E is the Earth's radius. This configuration is easily realized with the appropriate coordinate rotation. The ionosphere begins at an altitude $h = r_0 - R_E$ with a width d.

The signal path (Poynting vector) is refracted through the ionosphere with a direction of propagation that can be treated like a ray path under the geometric optics assumption [4, 3], which is valid for the frequency range of signals relevant to this report.

Consider an EM ray launched at an inclination angle of α at point $(R_E, \pi/2)$ as shown in Fig. 6(b), which intersects the satellite detector. We want to calculate the ray's total path S from its origin to the satellite detector

To begin, S_1 is calculated in terms of the underside pierce point P_0 located at x_0, y_0

$$S_1 = \frac{x_0}{\sin\alpha} \tag{36}$$

The radius from the origin to that point is given by the law of cosines

$$\begin{aligned} r_0^2 &= R_E^2 + S_1^2 - 2R_E S_1 \cos(\pi - \alpha) & (37)\\ &= R_E^2 + S_1^2 + 2R_E S_1 \cos(\alpha) & (38) \end{aligned}$$

Using equation 36, and $r_0 = R_E + h$, in equation 38 gives a quadratic equation for x_0 in terms of α

$$x_0 = -\frac{R_E}{2}\sin 2\alpha \pm \frac{1}{2}\sin 2\alpha \left[R_E^2 + \frac{h^2 + 2R_E h}{\cos^2\alpha}\right]^{1/2} \tag{39}$$

Discard the nonphysical (negative) root to get

$$x_0 = -\frac{R_E}{2}\sin 2\alpha + \frac{1}{2}\sin 2\alpha \left[R_E^2 + \frac{h^2 + 2R_E h}{\cos^2\alpha}\right]^{1/2} \tag{40}$$

and this is used in Eqn. 36 to find S_1.

Next, we need to find the initial incidence angle ψ_i of the ray at the point P_0. From the law of sines we have

$$\frac{R_E}{\sin\psi_i} = \frac{r_0}{\sin(\pi - \alpha)} \tag{41}$$

such that the incident underside pierce point angle is

$$\psi_i = \sin^{-1}\left(\frac{R_E}{r_0}\sin\alpha\right) \tag{42}$$

The initial transmission angle ψ_2 of the ray can be found from a local application of Snell's law at the underside pierce point P_0

$$\mathfrak{n}_0 \cdot \sin\psi_i = \mathfrak{n}_p(r_0)\sin\psi_2 \tag{43}$$

where the frequency dependence of $\mathfrak{n}_p$ is assumed, and $\mathfrak{n}_0 = 1$. Thus

$$\psi_2 = \sin^{-1}\left(\frac{1}{\mathfrak{n}_p(r_0)}\sin\psi_i\right) = \sin^{-1}\left(\frac{R_e}{r_0\mathfrak{n}_p(r_0)}\sin\alpha\right) \tag{44}$$

Now that we have found the initial transmission angle ψ_2, we will use the results of section 2.2.2 to calculate the ray's final location angle θ_1, Snell's law to find the transmission angle ψ_3 at the ionosphere topside, and the path S_2 through the ionosphere from points P_0 (bottom) to P_1 (top).

ψ is the angle between the ray's tangent and radial vector at any point inside the ionosphere shell, thus Bourger's law dictates that the expression

$$r\mathfrak{n}_p(r)\sin\psi(r) \;=\; r_0\mathfrak{n}_0\sin\psi_0 \;=\; K \tag{45}$$

is a constant. Also, from the differential triangle in Fig. 5(b)

$$\sin\psi = \frac{r\ d\theta}{dS} = \frac{r\ d\theta}{d\theta\left[r^2 + (dr/d\theta)^2\right]^{1/2}} \tag{46}$$

or equivalently, using Eq. 45

$$\frac{K}{r\mathfrak{n}_p(r)} = \frac{r\ d\theta}{d\theta\left[r^2 + (dr/d\theta)^2\right]^{1/2}} \tag{47}$$

Solve Eq. 47 for $d\theta/dr$

$$\frac{d\theta}{dr} = \frac{K}{r\left[r^2\mathfrak{n}_p^2(r) - K^2\right]^{1/2}} \tag{48}$$

and integrate to get the location angle at the topside

$$\theta_1 \;=\; \theta_0 \;-\; \int_{r_0}^{r_1=r_0+d} \frac{K}{r\left[r^2\mathfrak{n}_p^2(r) - K^2\right]^{1/2}}dr \tag{49}$$

where $\mathfrak{n}_0 = 1$ for vacuum on the bottom side, $K = r_0\sin\psi_i$, and the integral represents the parameter $\Delta\theta$ from Eqn. 32.

The incidence angle ψ_2' of the ray at the ionosphere topside at $P_1 = (r_1, \theta_1)$ is found from Eqn. 45 with $r = r_1$ and $\mathfrak{n}_0 = 1$

$$\sin\psi_2' = \frac{r_0\sin\psi_i}{r_1\mathfrak{n}(r_1)} \tag{50}$$

Application of Snell's law at that point gives

$$1\cdot\sin\psi_3 = \mathfrak{n}(r_1)\sin\psi_2' \tag{51}$$

Rearrange using Eqn. 50 to get the expression for the transmitted angle at P_1

$$\sin\psi_3 = \frac{r_0}{r_1}\sin\psi_i \tag{52}$$

The path length S_2 is found by integrating dS from r_0 to $r_1 = r_0 + d$. the differential path length dS is given by Eqn. 28

$$dS = \left[r^2 d\theta^2 + dr^2\right]^{1/2} = dr\left[1 + r^2\left(d\theta/dr\right)^2\right]^{1/2} \tag{53}$$

Using the expression for $d\theta/dr$ from Eqn. 48, we get

$$dS = \left[\frac{r^2\mathfrak{n}_p^2(r)}{r^2\mathfrak{n}_p^2(r) - K^2}\right]^{1/2} dr \tag{54}$$

Integrating this expression in r gives the path length S_2 through the ionosphere

$$S_2 = \int_{r_0}^{r_0+d} \frac{r\mathfrak{n}_p(r)}{\left[r^2\mathfrak{n}_p^2(r) - K^2\right]^{1/2}} dr \tag{55}$$

Finally, we need to calculate the path length S_3 from the ionospheric pierce point $P_1 = (r_1, \theta_1)$ to the satellite detector at $P_s = (r_s, \theta_s)$ in Fig. 6. Reference to Fig. 7 shows that

$$S_3 = \frac{\Delta x}{\cos\gamma} \tag{56}$$

Note that $\theta_1 = \psi_3 + \gamma$. Thus, the expression for S_3 is

$$S_3 = \frac{x_{sat} - x_1}{\cos(\theta_1 - \psi_3)} = \frac{x_{sat} - r_1\cos\theta_1}{\cos(\theta_1 - \psi_3)} \tag{57}$$

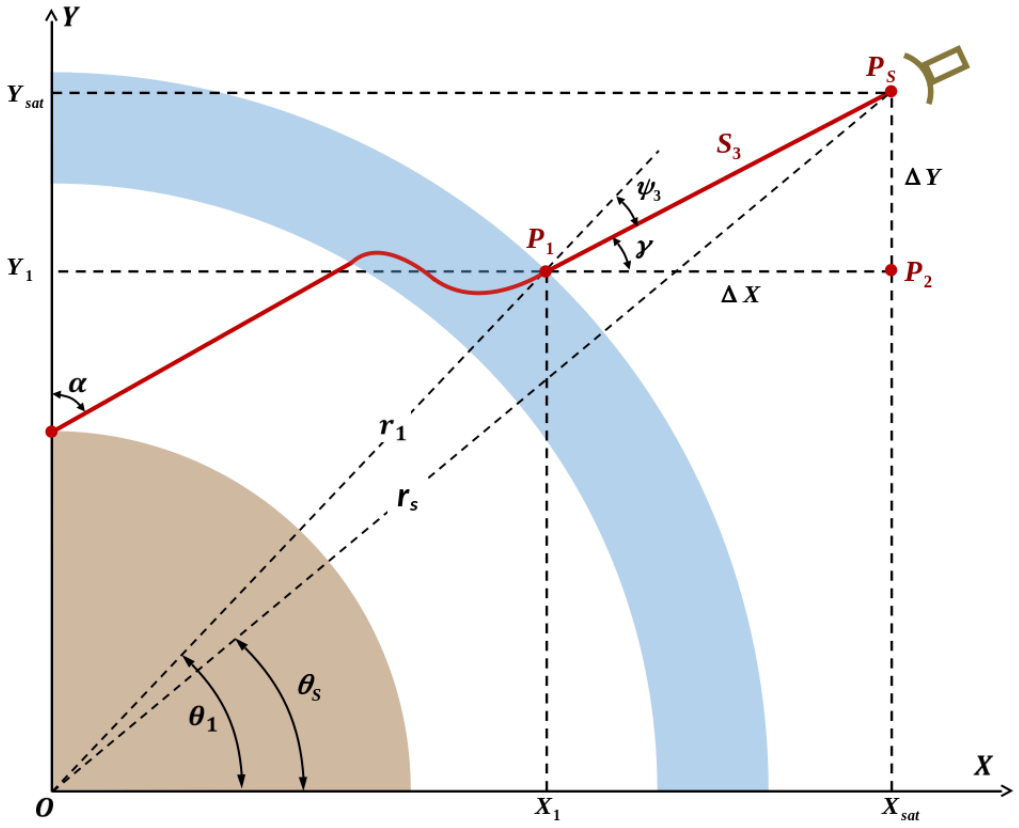

Figure 7: Showing the configuration for calculating the criterion.

Thus, given the satellite detector coordinates (r_S, θ_S), the ray that intersects the detector follows segments S_1, S_2, and S_3. These segment lengths are given in equations 36, 55, and 57. Note that first: all the parameters in those equations are functions of the launch angle α, and second: the detector location can be found in two ways. Consider the x coordinate. It is found from the detector coordinates

$$x_S = r_s \cos\theta_S \tag{58}$$

but can also be found using the derived expressions for the ray path

$$\begin{aligned} x_S &= x_1 + \Delta x \\ &= r_1 \cos\theta_1 + S_3 \cos\gamma \\ &= r_1 \cos\theta_1 + \frac{y_S - r_1 \sin\theta_1}{\tan(\theta_1 - \psi_3)} \end{aligned} \tag{59}$$

Equating the right hand side expressions in equations 58 and 59 results in a conditional equation that depends on α

$$r_s \cos\theta_S \stackrel{?}{=} r_1 \cos\theta_1(\alpha) + \frac{y_S - r_1(\alpha)\sin\theta_1(\alpha)}{\tan(\theta_1(\alpha) - \psi_3(\alpha))} \tag{60}$$

and will be called the constraint equation from here on. It is solved iteratively, at every frequency in the signal bandwidth, to find the launch angle α for the ray to intersect the satellite. Note that this angle may not exist depending on the detector position and parameters of the ionospere shell.

Each frequency component of the signal that intersects the detector will then have its amplitude decreased by a factor

$$\frac{1}{S_1 + S_2 + S_3}$$

The phase of those components is calculated using the phase delay time of the signal on each segment of the ray. The ray's phase velocity is the speed of light for segments S_1 and S_3 such that

$$\Delta t_{1,3} = \frac{S_{1,3}}{c} \tag{61}$$

The ray's phase delay in the ionosphere is given by the velocity of an EM wave in a magnetized plasma with the parameters specified by the ionosphere shell for segment S_2, that is

$$\Delta t_{iono} = \frac{S_2}{v_\phi} = \frac{S_2 \mathfrak{n}_p}{c} = \frac{1}{c} \int_{r_0}^{r_1} \frac{r \mathfrak{n}_p^2(r)}{\left[r^2 \mathfrak{n}_p^2(r) - K^2\right]^{1/2}} dr \tag{62}$$

4 solving the constraint equation

There are many methods for iteratively solving the constraint equation, 60. There are some important points to consider as well. From Fig. 7 and Snell's law at a vacuum/plasma interface, it is clear that any ray path originating from the point $(x, y) = (0, R_E)$ will refract in the clockwise direction at the underside of the ionosphere shell. This means that for the ray to intersect the detector, the maximum in α is defined as the angle between the y axis and the line of sight to the detector α_{SAT}, and this would be for no refraction in the ionosphere, so it is an absolute upper limit (see figure 8).

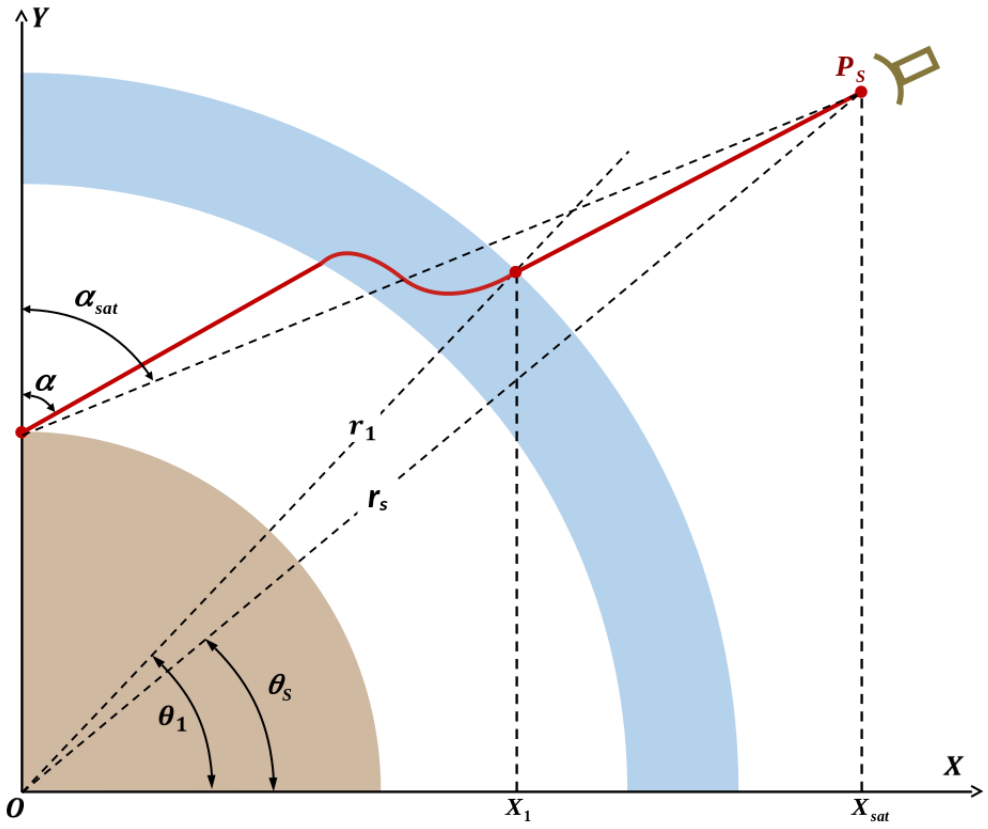

Figure 8: Geometry for the Snell's law shell model. Showing the relation between α and α_{SAT}.

The next item to consider is that once ψ_2 in figure 6(b) becomes equal to or greater than $\pi/2$, the ray has suffered complete reflection at the vacuum/plasma interface at the underside of the ionosphere shell. Thus $\psi_2(\alpha) < \pi/2$ for a ray to have a nonzero probability of reaching the detector. Equation 44 can be used in equation 42 to get

$$\psi_2(\alpha) \;=\; \sin^{-1}\left(\frac{R_e}{r_0\mathfrak{n}_p(r_0)}\sin\alpha\right) \;\leq\; \frac{\pi}{2} \tag{63}$$

or, in terms of the angle α

$$\alpha \leq \sin^{-1}\left(\frac{r_0\mathfrak{n}_p(r_0)}{R_e}\right) \tag{64}$$

Equations 63 and 64 define the upper limit on the angle α, whichever is smaller. The α root that solves the constraint equation can be bracketed in the interval

$$\begin{aligned} [0,\ \alpha_{SAT}] \quad &, \quad \alpha_{SAT} < \sin^{-1}\left(\frac{r_0\mathfrak{n}_p(r_0)}{R_e}\right) \\ \left[0,\ \sin^{-1}\left(\frac{\mathfrak{n}_p R_0}{R_E}\right)\right] \quad &, \quad \alpha_{SAT} \geq \sin^{-1}\left(\frac{r_0\mathfrak{n}_p(r_0)}{R_e}\right) \end{aligned}$$

References

[1] M. Light, "The snell's law shell ionospheric transfer function." Los Alamos National Laboratory report LA-UR-24414.

[2] F. G. Stremler, *Introduction to Communication Systems*. Addison-Wesley, second ed., 1982.

[3] K. G. Budden, *The Propagation of Radio Waves*. Cambridge University Press, 1985.

[4] D. G. Swanson, *Plasma Waves*. Institute of Physics, second ed., 2003.

[5] G. B. Thomas, *Calculus and Analytic Geometry*. Addison-Wesley, third ed., 1966.